CHEMISTRY
A EUROPEAN JOURNAL

DOI: 10.1002/chem.200700936

Face-to-Face Pacman-Type Porphyrin–Fullerene Dyads: Design, Synthesis, Charge-Transfer Interactions, and Photophysical Studies

Francis D'Souza,*[a] Eranda Maligaspe,[a] Paul A. Karr,[a] Amy Lea Schumacher,[a] Maya El Ojaimi,[b] Claude P. Gros,[b] Jean-Michel Barbe,*[b] Kei Ohkubo,[c] and Shunichi Fukuzumi*[c]

Abstract: Pacman-type face-to-face zinc–porphyrin–fullerene dyads have been newly synthesized and studied. Owing to the close proximity of the donor and acceptor entities, strong π–π intramolecular interactions between the porphyrin and fullerene entities resulted in modulating the spectral and electrochemical properties of the dyads. New absorption and emission bands that correspond to the charge-transfer interactions were observed in the near-IR region. Time-resolved transient absorption studies revealed efficient photoinduced electron transfer from the singlet excited porphyrin to the fullerene entity. The rate constants for photoinduced electron transfer are analyzed in terms of the Marcus theory of electron transfer, which afforded a large electron coupling matrix element ($V = 140\,\mathrm{cm}^{-1}$) for the face-to-face dyads. As a consequence of the large charge-recombination driving force in the Marcus inverted region, a relatively long lifetime of the charge-separated state has been achieved.

Keywords: charge transfer · electron transfer · fullerenes · photosynthesis · porphyrinoids

Introduction

Molecular and supramolecular donor–acceptor dyads capable of undergoing light-induced energy and electron transfer have been widely studied as mimics of natural photosynthetic reaction centers and as photochemical molecular devices.[1–12] The composition, interchromophore distance and orientation, and electronic coupling are important factors in modulating the electron-transfer efficiency and the lifetime of the charge-separated state.[2–12] To achieve efficient intramolecular electron-transfer processes, both covalent chemistry and biomimetic self-assembly methodologies, such as the formation of π stacks, hydrogen bonds, and van der Waals contacts, have been successfully utilized to connect the donor–acceptor entities.[2–12] In the majority of these studies, porphyrins or phthalocyanines have been used as photosensitizers and a variety of electron acceptors have been employed. Among the different electron acceptors employed, fullerene C_{60} has become the ultimate electron acceptor owing to favorable reduction potentials and small reorganization energies in electron-transfer reactions.[4–12] As a consequence, C_{60} promotes photoinduced charge separation (CS), but retards the charge-recombination (CR) process, which results in the formation of much desired long-lived charge-separated states.[4–12] Several comprehensive reviews of the literature of donor–fullerene dyads, which includes larger hybrids (triads, tetrads, pentads, etc.), that incorporate a wide variety of electron donors and linkers have been published.[2–6]

To get more insight into the influence of molecular topology on electron transfer, a few porphyrin–fullerene dyads in which the π systems are structurally forced into a face-to-

---

[a] Prof. F. D'Souza, E. Maligaspe, Prof. P. A. Karr, A. L. Schumacher
Department of Chemistry, Wichita State University
1845 Fairmount, Wichita, Kansas 67260–0051 (USA)
Fax: (+1) 316-978-3431
E-mail: Francis.DSouza@wichita.edu

[b] M. El Ojaimi, Dr. C. P. Gros, Dr. J.-M. Barbe
ICMUB, UMR 5260, Université de Bourgogne
9, Avenue Alain Savary, BP 47870
21078 Dijon Cedex (France)
Fax: (+33) 380-396-117
E-mail: Jean-Michel.Barbe@u-bourgogne.fr

[c] Dr. K. Ohkubo, Prof. S. Fukuzumi
Department of Material and Life Science
Graduate School of Engineering, Osaka University
SORST, Japan Science and Technology Agency,
Suita, Osaka, 565-0871 (Japan)
Fax: (+81) 6-6879-7370
E-mail: fukuzumi@chem.eng.osaka-u.ac.jp

Supporting information for this article is available on the WWW under http://www.chemeurj.org/ or from the author. It contains transient absorption spectra and the decay profiles of **1** and **3** after femtosecond laser pulse irradiation in toluene.

face arrangement have been elegantly designed and studied. Two types of dyads, namely, porphyrin–fullerene cyclophane dyads (Scheme 1a), which were synthesized independently by the groups of Diederich and Hirsch,[13] and porphyrin–fullerene parachute dyads synthesized by Schuster and co-workers (Scheme 1b),[14] are well known.

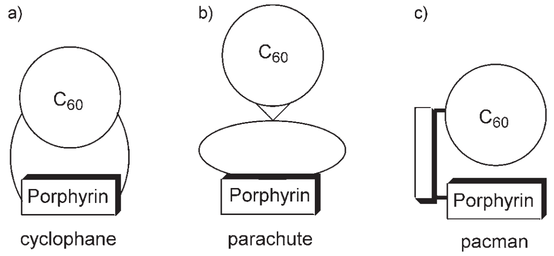

Scheme 1. Examples of closely held porphyrin–fullerene dyads.

For the synthesis of these dyads, tethers with terminal malonate moieties were attached at the *meta* positions of the 5,15-phenyl rings of a tetraphenylporphyrin precursor. In addition, supramolecular systems that employ multiple modes of binding to attain defined distances and orientations have also been reported.[5–8] Additionally, a few dyads with porphyrin and fullerene entities positioned face-to-face, but with relatively more structural flexibility are also known.[15]

In the present study, we wish to report a series of Pacman-type face-to-face porphyrin–fullerene dyads of the type shown in Scheme 1c. In these dyads, the porphyrin and fullerene entities are held closely together by either flexible or rigid spacers (Scheme 2). It may be mentioned here that the Pacman-type approach employed has been one of the successful approaches used to obtain closely held porphyrin–porphyrin dimers in the literature.[16–19] Owing to the nature of the spacer, the present porphyrin–fullerene dyads are expected to be structurally more rigid compared with the dyads shown in Scheme 1a and b.

Results and Discussion

Synthesis of the Pacman porphyrin–fullerene dyads was accomplished first by synthesizing a porphyrin with an aldehyde-functionalized spacer at the *meso* position.[18] Subsequently, the aldehyde group was treated with C_{60} and sarcosine by using the standard Prato method for fulleropyrrolidine synthesis.[20] The structural integrity of the newly synthesized dyads was established by UV-visible and NMR spectroscopies, mass spectrometry, and electrochemical methods.

Ground-state charge-transfer interactions: The optical absorption spectrum of dyad **1** and the reference compounds, recorded separately for the Soret and visible regions, are shown in Figure 1. The zinc–porphyrin (ZnP) with a *meso*-substituted spacer group (compounds **1**–**3** in the absence of a fullerene unit) and a zinc–octaethylporphyrin (ZnOEP) were used as reference compounds. The dyads have a band at around $\lambda = 330$ nm that corresponds to the fulleropyrrolidine entity. The Soret band of the dyads was red-shifted by 8 to 15 nm compared with the reference compounds. Such a trend was also observed for the positions of the visible bands. Interestingly, in the near-IR portion of the spectrum, which includes the region from 600 to 800 nm, a broad ab-

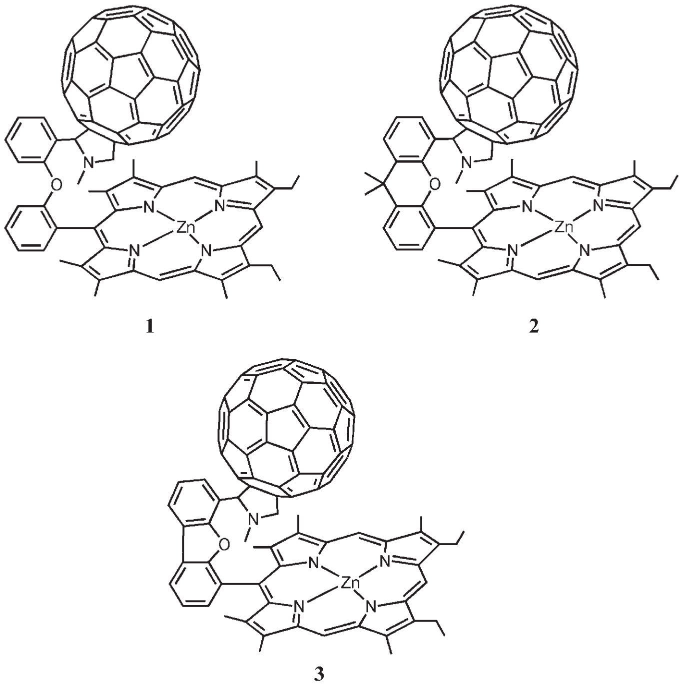

Scheme 2. Examples of Pacman-type porphyrin–fullerene dyads with rigid or flexible spacers.

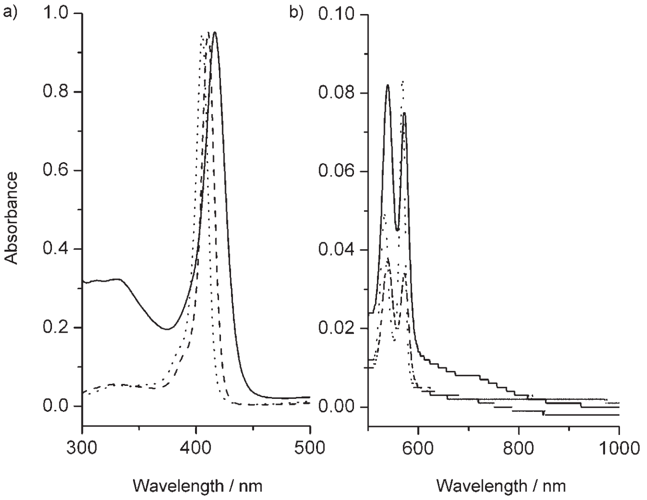

Figure 1. UV-visible spectrum of dyad **1** (——), Pacman porphyrin reference (-----), and zinc–octaethylporphyrin (•••••) in *o*-dichlorobenzene. The concentration was held at 2.7 mM. The broad absorption of **1** in the 600–800 nm region is attributed to the charge-transfer interactions.

sorption was observed for these dyads. Based on the results of earlier reports, this band was attributed to the charge-transfer interactions between the two π entities.[21,22]

Further computational studies were performed at the B3LYP/3-21G(*) level[23] to visualize the geometry and electronic structure of the dyads. For these computational studies the molecules were optimized on a Born–Oppenheimer potential-energy surface and a global minimum was obtained for each of these dyads. The structures of two such dyads, **1** and **2**, are shown in Figure 2, in which a face-to-face orientation of the porphyrin and fullerene entities was clearly observed. The distance between zinc and the closest carbon of the fullerene spheroid were around 2.2 to 2.3 Å, which indicates that the donor and acceptor entities were within distances suitable for van der Waals interactions. It is important to note that in the case of the flexibly linked dyad (**1**) this distance was as close as that of dyads with rigid spacers. This could be attributed to the spontaneous attraction between the porphyrin and fullerene entities that was further structurally supported by the small spacer unit.[22]

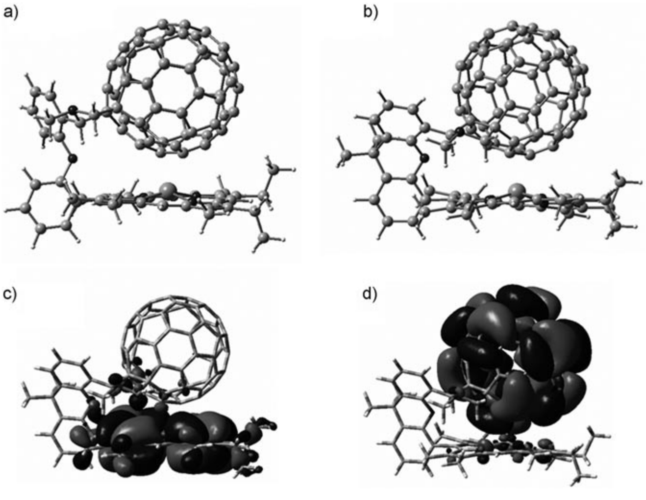

Figure 2. B3LYP/3-21G(*) optimized structures of **1** (a) and **2** (b). The frontier HOMO (c) and LUMO of **2** (d) are also shown.

The frontier HOMOs and LUMOs generated at the B3LYP/3-21G(*) level were also suggestive of charge-transfer-type interactions in the ground state of the dyads. As predicted, a large majority of the HOMO was located on the porphyrin π system, whereas the majority of the LUMO was located on the fullerene spheroid for all of the dyads studied. However, a small fraction of the HOMO was located on the fullerene entity and a small fraction of the LUMO was located on the porphyrin entity. Earlier, such partial delocalization of the frontier orbitals was attributed to the ground-state charge-transfer-type interactions between the donor and acceptor entities.[15b,23] As the majority of the HOMO was on the porphyrin and the majority of the LUMO was on the fullerene, a $ZnP^{\bullet+}$–$C_{60}^{\bullet-}$ charge-separated state could be visualized during photoinduced electron transfer in these dyads. The HOMO–LUMO gap calculated in the gas phase was found to range from 1.68 to 1.79 eV for these dyads, which were comparable to the HOMO–LUMO gaps reported in the literature for related ZnP–fullerene dyads.[21]

Electrochemical studies conducted by using cyclic voltammetry techniques were performed to evaluate the redox potentials of the newly synthesized dyads. These measurements were important because the ZnP unit in the present series of dyads had different substituents compared with the zinc–tetraphenylporphyrin (ZnTPP) macrocycle that is traditionally used. Figure 3 shows cyclic voltammograms for **3**, whereas the redox potentials for all of the dyads studied, along with the values for reference compounds, are given in Table 1. The ZnP unit exhibited the expected two one-elec-

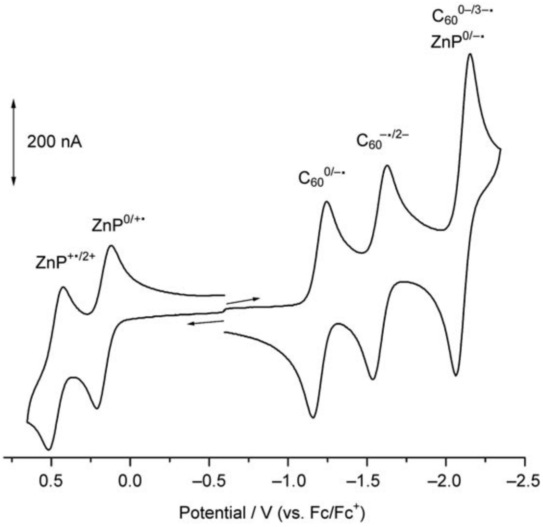

Figure 3. Cyclic voltammogram of **3** in PhCN with 0.1 M $(n\mathrm{Bu})_4\mathrm{NClO}_4$. Scan rate = 0.1 V s^{-1}. The concentration of the dyad was ≈0.1 mM.

Table 1. Electrochemical redox potentials (E, V vs. Fc/Fc$^+$), and free-energy changes for photoinduced electron transfer (ΔG_{RIP}) and charge separation (ΔG_{CS}) for the dyads in benzonitrile.[a]

Compound	Zn–C[b] [Å]	$ZnP^{\bullet+/2+}$	$ZnP^{0/\bullet+}$	$C_{60}^{0/\bullet-}$	$C_{60}^{\bullet-/2-}$	$C_{60}^{2-/3-}$ $ZnP^{0/\bullet-}$	$-\Delta G_{\mathrm{RIP}}$[e] [eV]	$-\Delta G_{\mathrm{CS}}$[f] [eV]
1	2.20	0.46	0.15	−1.23	−1.60	−2.15[c]	1.38	0.72
2	2.24	0.50	0.18	−1.23	−1.68	−2.21[c]	1.41	0.69
3	2.21	0.47	0.17	−1.20	−1.58	−2.11[c]	1.37	0.73
$\mathbf{1}_{\mathrm{ref}}$	–	0.47	0.17	–	–	−2.09[d]	–	–
$\mathbf{2}_{\mathrm{ref}}$	–	0.45	0.16	–	–	−2.11[d]	–	–
$\mathbf{3}_{\mathrm{ref}}$	–	0.48	0.17	–	–	−2.08[d]	–	–
ZnOEP	–	0.51	0.18	–	–	−2.14[d]	–	–

[a] see Scheme 1 for structures; reference compounds are porphyrins with the *meso* spacer unit. [b] Distance between zinc and closest C_{60} carbon. [c] Overlap of the first reduction of porphyrin and the third reduction of fullerene (two one-electron processes). [d] Corresponds to the first reduction of porphyrin. [e] $\Delta G_{\mathrm{RIP}} = e(E_{\mathrm{ox}} - E_{\mathrm{red}})$, in which the Coulombic interaction in a polar solvent (PhCN) is neglected. [f] $-\Delta G_{\mathrm{CS}} = \Delta E_{0\text{-}0} - \Delta G_{\mathrm{RIP}}$, in which $\Delta E_{0\text{-}0}$ is the energy of the lowest ZnP excited state.

tron oxidations and two one-electron reductions while up to three one-electron reductions that corresponded to the reduction of fulleropyrrolidine were also observed within the potential window of the solvent. The oxidation of the ZnP unit in these dyads was found to be easier by over 100 mV compared with ZnTPP. However, they were 20 to 30 mV more difficult to oxidize compared with the ZnP reference that contained the *meso* spacer group. The first cathodic process corresponding to the reduction of the fullerene entity was located at approximately −1.20 V versus Fc/Fc$^+$, and was cathodically shifted by 20 to 30 mV compared with pristine fulleropyrrolidine. The small anodic shift of the ZnP oxidation and the small cathodic shift of the fulleropyrrolidine reduction compared with their reference compounds are indicative of charge-transfer-type interactions between them. That is, the charge-transfer interactions make ZnP oxidation and fullerene reduction slightly more difficult.

The experimentally measured HOMO–LUMO gap (the potential difference between the first oxidation of ZnP and the first reduction of fullerene) was found to range from 1.37 to 1.46 V. These values are comparable to ZnP–fullerene dyads in the literature, but slightly lower than that estimated by molecular orbital calculations in the gas phase. The free-energy changes of CS (ΔG_{CS}) were calculated according to the Rehm and Weller method[24] by employing the first oxidation potential of ZnP, the first reduction potential of C_{60}, the singlet excitation energy of ZnP, and the estimated Coulomb energy. The ΔG_{CS} values for generating ZnP$^{\bullet+}$–C$_{60}^{\bullet-}$ radical ion pairs, were found to range from −0.69 to −0.73 eV (Table 1), which indicated that the occurrence of photoinduced CS from singlet excited ZnP to the C_{60} entity was an exergonic process.

The above studies clearly suggest the existence of charge-transfer-type interactions between electron-rich ZnP and electron-deficient fullerene in the face-to-face dyads. It is important to note that such interactions resulted in modulating the optical and electrochemical properties. Further studies that involve steady-state and time-resolved emission techniques were performed to probe excited-state electron transfer in these dyads.

Steady-state emission studies: Figure 4 shows the fluorescence spectrum of **1** along with the reference compounds. The dyads had two emission bands at around $\lambda = 575$ and 626 nm that correspond to the ZnP entity, however, with much diminished intensities compared to the intensities of the reference compounds (over 90 % quenching compared with the ZnOEP reference compound). These results indicate the occurrence of excited-state events in the dyads. Attempts were also made to locate the charge-transfer emission bands of the dyads. The inset of Figure 4 shows that a weak band at around $\lambda = 825$ nm was observed when the dyads were excited at 680 nm, which corresponds to the charge-transfer absorption band. The emission band was better defined in polar solvents, such as DMF or benzonitrile, than in less polar solvents, such as *o*-dichlorobenzene. Excitation of the charge-transfer band did not result in the formation of new bands that correspond to exciplex formation, perhaps owing to its low ε values.

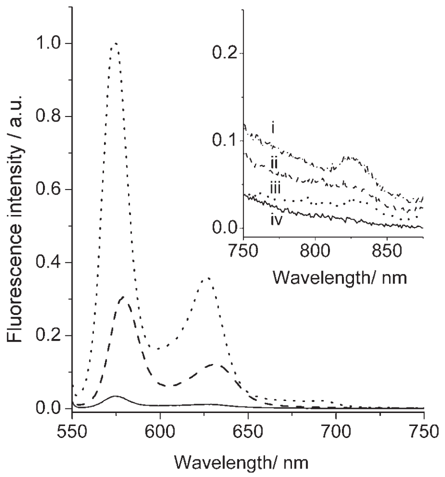

Figure 4. Fluorescence spectrum of **1** (——), Pacman porphyrin reference (-----), and ZnOEP (•••••) in *o*-dichlorobenzene. The porphyrin concentrations were held at 2.7 mM and the samples were excited at the most intense visible band. The inset shows the charge-transfer emission in the near-IR region in DMF (i), benzonitrile (ii), acetonitrile (iii), and *o*-dichlorobenzene (iv). $\lambda_{ex} = 680$ nm corresponds to the charge-transfer absorption band.

Transient absorption measurements: Time-resolved transient absorption spectra of **1**–**3** were observed by femtosecond laser flash photolysis in deaerated PhCN, as shown in Figure 5. The absorption band observed at $\lambda = 1000$ nm in each case is a clear attribute of the monofunctionalized fullerene radical anion.[8–12] The accompanying absorption band at 675 nm agrees with that of the ZnP π radical cation.[8–12] Thus, the transient absorption spectra shown in Figure 5 indicate the formation of the radical ion pair state (ZnP$^{\bullet+}$–C$_{60}^{\bullet-}$) for **1**, **2**, and **3** in PhCN.

The CS rate constants (k_{CS}, Table 2) for the formation of the radical ion pairs were determined from the rise in the absorbance at 1000 nm due to $C_{60}^{\bullet-}$ to be 2.4×10^{12} s^{-1} for **1** (Figure 6a), 9.5×10^{11} s^{-1} for **2** (Figure 6c), and 1.5×10^{12} s^{-1} for **3** (Figure 6e). These rates were found to be one or two orders of magnitude higher than those reported for a number of porphyrin–fullerene dyads in the literature.[12–15] From the CS rates, the quantum yields of the charge-separated state are estimated to be almost 100 %.

The decay rate constants (k_{CR}) of the radical ion pairs are determined from the decay in absorbance at 1000 nm as 6.5×10^{10} s^{-1} for **1** (Figure 6b), 5.0×10^{10} s^{-1} for **2** (Figure 6d), and 5.2×10^{10} s^{-1} for **3** (Figure 6f). Back electron transfer in the radical ion pair occurs to produce the ground state rather than the triplet excited state of C_{60} because the charge-separated state energy is lower than the triplet energy of C_{60} in PhCN. In fact, no C_{60} triplet was observed in the nanosecond laser flash photolysis measurements of the dyads in PhCN.

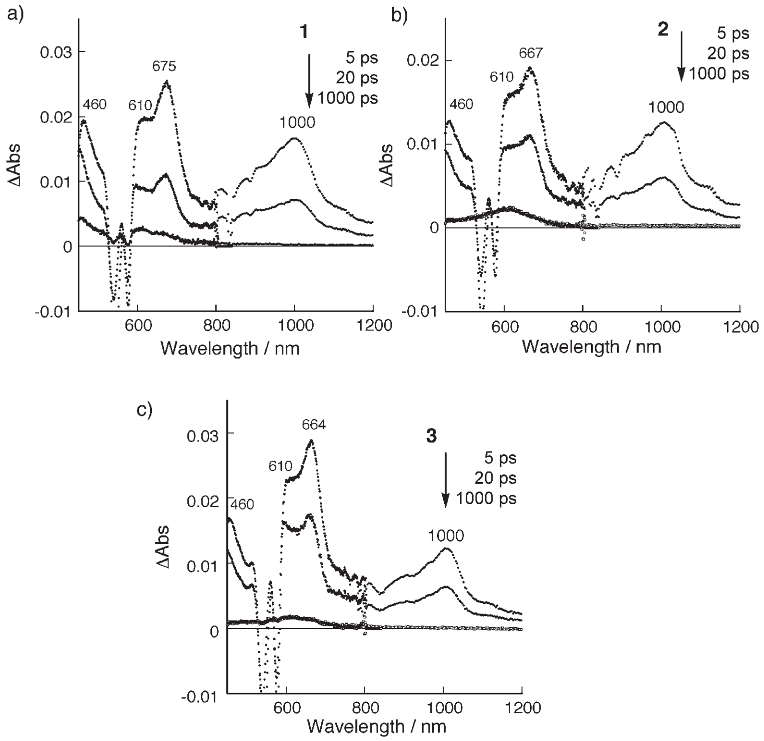

Figure 5. Transient absorption spectra of **1** (a), **2** (b), and **3** (c) recorded 5, 20, and 1000 ps after femtosecond laser pulse irradiation at 410 nm in PhCN at 298 K.

Table 2. Values for k_{CS}, the lifetime for CS, k_{CR}, and the lifetime of radical ion pair (τ_{RIP}) of the dyads in benzonitrile and toluene.

Compound	Solvent	k_{CS}[a] [s^{-1}]	τ_{CS}[a] [ps]	k_{CR}[b] [s^{-1}]	τ_{RIP}[b] [ps]
1	PhCN	2.4×10^{12}	0.42	6.5×10^{10}	15
	Toluene	6.8×10^{10}	14	19×10^{10}	520
2	PhCN	9.5×10^{11}	1.1	5.0×10^{10}	20
	Toluene	3.5×10^{11}	29	2.6×10^{9}	380
3	PhCN	1.5×10^{12}	0.67	5.2×10^{10}	19
	Toluene	5.2×10^{10}	19	2.3×10^{9}	430

[a] From the rise rate at 1000 nm. [b] From the decay rate at 1000 nm.

To quantify the driving-force dependence on the electron-transfer rate constants (k_{ET}), Equation (1) was used, in which V is the electronic coupling matrix element, k_B is the Boltzmann constant, h is the Planck constant, and T is the absolute temperature.[25]

$$k_{ET} = \sqrt{\frac{4\pi^3}{h^2\lambda k_B T}}\, V^2 \exp\left[-\frac{(\Delta G^0{}_{ET}+\lambda)^2}{4\lambda k_B T}\right] \qquad (1)$$

Figure 7 shows the driving-force dependence of $\log k_{ET}$ (k_{CS} and k_{CR}) for the CS and CR of **1**, **2**, and **3** in PhCN at 298 K. The solid line is drawn as the best fit line by using the values of $\lambda = 0.94$ eV and $V = 140\ cm^{-1}$. The large V value is consistent with adiabatic electron transfer with a close distance between the ZnP and the C_{60} moieties in **1**, **2**, and **3**. As the driving force of CR is larger than the λ value (0.94 eV), the CR process lies in the Marcus inverted region, in which larger driving forces result in smaller electron-transfer rate constants.[25]

The overall λ value (0.94 eV) for the present dyads is significantly larger than the value (0.66 eV) reported for the ZnTTP–C_{60} dyad with an edge-to-edge distance (R_{ee}) of 11.9 Å.[26] The R_{ee} values between ZnP and C_{60} in **1**, **2**, and **3** are evaluated to be 2.20, 2.24, and 2.21 Å, respectively, from the optimized structures. In general, the smaller the R_{ee} value the smaller the solvent reorganization energy will be, as expected from the Marcus theory of electron transfer.[25] Thus, the relatively large λ value may result from the significant interaction between closely positioned $ZnP^{\bullet+}$ and $C_{60}^{\bullet-}$ in the charge-separated states. The large λ value is also consistent with the existence of charge-transfer-type interactions between electron-rich ZnP and electron-deficient fullerene in the face-to-face dyads (see above).

The charge-separated state of the dyads was also observed in toluene, which is much less polar than PhCN, as shown in Figure 8a for **2**.[27] The rate constant for the formation of the charge-separated state was determined from the rise in the absorbance at 1000 nm due to $C_{60}^{\bullet-}$ (Figure 8b), which is much smaller than the corresponding values recorded in PhCN (Table 2). The k_{CS} value, which was determined from the decay in the absorbance at 1000 nm (Figure 8c), was found to be an order of magnitude smaller than the corresponding values in PhCN (Table 2; see the Supporting Information for the data for **1** and **3**). The smaller k_{CS} value may result from the smaller driving force of CS in toluene than that in PhCN because the CS process is in the Marcus normal region in Figure 7. On the other hand, the larger CR driving force in toluene may result in the smaller CR rate constant in the Marcus inverted region (Figure 7). It was confirmed that no C_{60} triplet was observed in the nanosecond laser flash photolysis measurements of **2** in toluene. This observation indicates that back electron transfer to the ground state is faster than that to the triplet excited state of C_{60} in toluene.

The formation of relatively long-lived charge-separated states in nonpolar solvent is an important feature of the present series of Pacman porphyrin–fullerene dyads. Although literature examples of porphyrin–fullerene dyads that do not have strong charge-transfer interactions yielded charge-separated states in polar solvents,[3–6] in a nonpolar

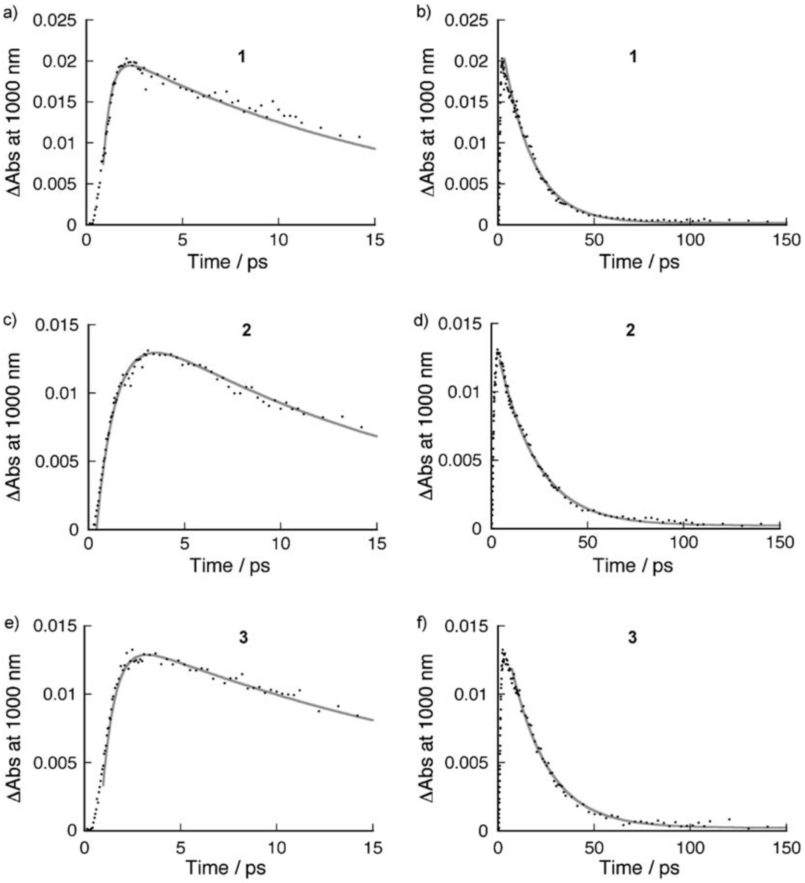

Figure 6. Time profiles of absorbance at 1000 nm for **1** at 0–15 (a) and 0–150 ps (b), **2** at 0–15 (c) and 0–150 ps (d), and **3** at 0–15 (e) and 0–150 ps (f) time intervals. The gray curves represent the best fit to the two-exponential rise and decay.

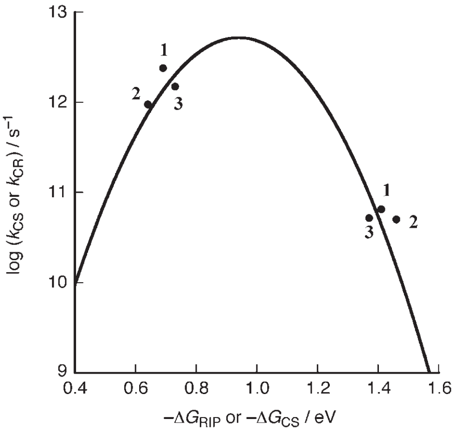

Figure 7. Driving force ($-\Delta G_{RIP}$ or $-\Delta G_{CS}$) dependence on the intramolecular ET rate constants (k_{CS} or k_{CR}) for the dyads investigated in PhCN. The curve represents the best fit to Equation (1) to give $\lambda = 0.94$ eV and $V = 140$ cm^{-1}.

solvent only the population of the triplet state was observed.[27] Owing to the close proximity and the resulting strong charge-transfer-type interactions between the donor and acceptor entities in the Pacman porphyrin–fullerene dyads, it was possible to modulate the energy states that ultimately result in CS in a nonpolar solvent. A similar observation was made for a parachute-type porphyrin–fullerene dyad,[14b] however, the charge-separated state is lower than the triplet excited state in the present series of dyads. Finally, the face-to-face geometry and the comparison of the V values of the present dyads with other dyads in the literature indicates that through-space orbital interactions may play a major role in the adiabatic electron-transfer processes, as indicated by the Marcus plot shown in Figure 7.

Conclusion

A series of closely held porphyrin–fullerene dyads with face-to-face orientation have been reported. Spectral and electrochemical studies indicated the existence of charge-transfer interactions between electron-rich ZnP and electron-deficient fullerene in these dyads. The face-to-face geometry of the dyads resulted in the observation of efficient photoinduced electron transfer from the singlet excited state of the ZnP moiety to the C_{60} moiety with a large electron coupling matrix element ($V = 140$ cm^{-1}) to produce the charge-separated state.[28] A relatively long lifetime of the charge-separated state has been achieved in toluene because of the large CR driving force in the Marcus inverted region. This is in sharp contrast to a number of porphyrin–fullerene dyads reported in the literature (with the exception of the parachute-type porphyrin–fullerene dyad mentioned above[14b]), in which population of the triplet state, instead of CS, has been the common excited-state deactivation mechanism in nonpolar solvents.[29]

Experimental Section

Chemicals: All solvents and reagents were used as received. Tetra-*n*-butylammonium perchlorate was obtained from Fluka Chemicals. The syntheses of ZnOEP and ZnP with a *meso* spacer unit were carried out according to literature procedures.[18]

Synthesis of 13,17-diethyl-2,3,7,8,12,18-hexamethyl-5-[8-(fulleropyrrolidine) diphenyl ether] (1): A solution of C_{60} (20 mg, 0.027 mmol), *N*-methylglycine (4.9 mg, 0.055 mmol), and diphenyl ether bridged porphyrin al-

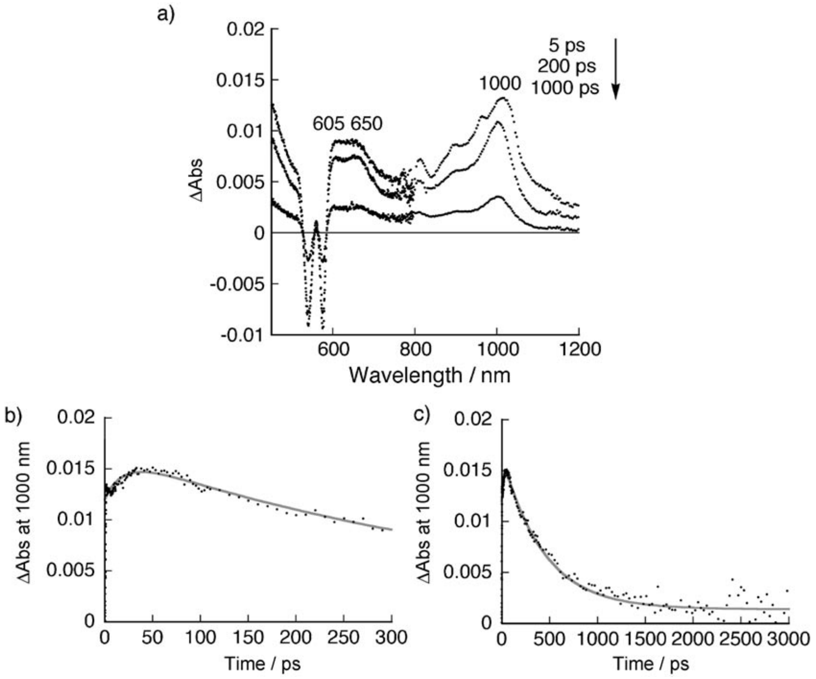

Figure 8. a) Transient absorption spectra of **2** taken at 5, 200, and 1000 ps after femtosecond laser pulse irradiation at 410 nm in toluene at 298 K. Time profiles of absorbance at 1000 nm for **2** at 0–300 (b) and 0–3000 ps (c) time intervals. The gray curves represent the best fit to the two-exponential rise and decay.

dehyde (59.2 mg, 0.055 mmol) in toluene (100 mL) was heated at reflux for 6 h before the solvent was evaporated. The crude product was purified by column chromatography (silica gel, hexane/toluene 45:55) to give the product (22 mg, 55 %). ^{1}H NMR (300 MHz, $CDCl_3$): $\delta = 9.98$ (s, 1H), 9.90 (s, 1H), 9.81 (s, 1H), 8.14 (dd, $J = 7.8$ Hz, 1H), 7.77 (t, $J = 7.8$ Hz, 2H), 7.52–7.58 (m, 1H), 7.31–7.33 (m, 2H), 7.20–7.30 (m, 2H), 4.75 (s, 1H), 4.21 (dd, $J = 9.01$ Hz, 2H), 4.00–4.10 (m, 4H), 3.65 (s, 3H), 3.50 (s, 3H), 3.48 (s, 3H), 3.43 (s, 3H), 2.82 (s, 3H), 2.75 (s, 3H), 2.68 (s, 3H), 1.95 (t, $J = 7.5$ Hz, 3H), 1.77 ppm (t, $J = 7.5$ Hz, 3H); UV/Vis (PhCN): $\lambda_{max} = 330.0$, 416.6, 538.8, 571.6 nm; MS (MALDI-TOF): m/z: 1457.8 $[M]^+$.

Synthesis of 13,17-diethyl-2,3,7,8,12,18-hexamethyl-5-[8-(fulleropyrrolidine)-9,9-dimethyl-9H-xanthene] (2): A solution of C_{60} (40 mg, 0.083 mmol), *N*-methylglycine (10 mg, 0.11 mmol), and pyran bridged porphyrin aldehyde (40 mg, 0.055 mmol) in toluene (100 mL) was heated at reflux for 6 h before the solvent was evaporated. The crude product was purified by column chromatography (silica gel, hexane/toluene 55:45) to give the product (11.0 mg, 28.1 %). ^{1}H NMR (300 MHz, $CDCl_3$): $\delta = 10.25$ (s, 1H), 9.90 (s, 1H), 9.81 (s, 1H), 8.14 (d, $J = 7.8$ Hz, 1H), 7.88 (d, $J = 7.8$ Hz, 1H), 7.68–7.70 (m, 2H), 7.50 (d, $J = 7.8$ Hz, 1H), 7.35 (d, $J = 7.7$ Hz, 1H), 5.30 (s, 1H), 4.20–4.30 (m, 4H), 4.19 (dd, $J = 9.0$ Hz, 2H), 3.70 (s, 3H), 3.57 (s, 3H), 3.49 (s, 3H), 3.28 (s, 3H), 2.48 (s, 3H), 2.23 (s, 3H), 2.07 (s, 3H), 1.80 ppm (t, $J = 7.5$ Hz, 6H); UV/Vis (PhCN): $\lambda_{max} = 326.1$, 415.5, 538.5, 573.1 nm; MS (MALDI-TOF): m/z: 1497.5 $[M]^+$.

Synthesis of 13,17-diethyl-2,3,7,8,12,18-hexamethyl-5-[8-(fulleropyrrolidine)dibenzofuran] (3): A solution of C_{60} (75 mg, 0.105 mmol), *N*-methylglycine (12.5 mg, 0.140 mmol), and furan bridged porphyrin aldehyde (52.5 mg, 0.072 mmol) in toluene (100 mL) was heated at reflux for 6 h before the solvent was removed in vacuo. The residue was purified by column chromatography (Silica gel, hexane/toluene 40:60) to give the product (27 mg, 25.4 %). ^{1}H NMR (300 MHz, $CDCl_3$): $\delta = 10.18$ (s, 1H), 9.98 (s, 1H), 9.92 (s, 1H), 8.35 (d, $J = 7.4$ Hz, 1H), 8.11 (d, $J = 7.8$ Hz, 1H), 8.06 (d, $J = 7.5$ Hz, 1H), 7.93 (d, $J = 7.4$ Hz, 1H), 7.74 (t, $J = 7.3$ Hz, 1H), 7.51 (t, $J = 7.4$ Hz, 1H), 4.84 (s, 1H), 4.19 (dd, $J = 9.4$ Hz, 2H), 4.08–4.15 (m, 4H), 3.66 (s, 3H), 3.39 (s, 3H), 2.56 (s, 3H), 2.50 (s, 3H), 2.40 (s, 3H), 2.29 (s, 3H), 1.87 (t, $J = 7.5$ Hz, 6H), 1.80 ppm (s, 3H); UV/Vis (PhCN): $\lambda_{max} = 329.1$, 412.1, 536.9, 572.1 nm; MS (MALDI-TOF): m/z: 1454.7 $[M]^+$.

Methods and instrumentation: ^{1}H NMR spectra were recorded for solutions in $CDCl_3$ by using a Varian 400 MHz NMR spectrometer with tetramethylsilane as the internal standard. The UV/Vis spectral measurements were carried out by using a Shimadzu Model 1600 UV/Vis spectrophotometer. The fluorescence emission was monitored by using a Varian Eclipse spectrometer. Cyclic voltammograms were recorded by using an EG&G Model 263 A potentiostat with a three electrode system. A platinum button electrode was used as the working electrode. A platinum wire served as the counter electrode and Ag/AgCl was used as the reference electrode. An Fc/Fc^+ redox couple was used as an internal standard. All of the solutions were purged prior to electrochemical and spectral measurements by using argon gas. The computational calculations were performed by DFT B3LYP/3-21G(*) methods[23] with the GAUSSIAN 03[30] software package on high-speed computers. To generate the frontier orbitals, the GaussView[30] program was used.

Time-resolved transient absorption measurements: Femtosecond laser flash photolysis was conducted by using a Clark-MXR 2010 laser system and an optical detection system provided by Ultrafast Systems (Helios). The source for the pump and probe pulses were derived from the fundamental output of a Clark laser system (775 nm, 1 mJ per pulse, fwhm = 150 fs) at a repetition rate of 1 kHz. A second harmonic generator introduced in the path of the laser beam provided laser pulses at $\lambda = 410$ nm for excitation. The second harmonic was generated by using 95 % of the fundamental output of the laser, whereas 5 % of the deflected output was used for the generation of white light. Prior to generating the probe continuum, the laser pulse was fed to a delay line that provided an experimental time window of 1.6 ns with a maximum step resolution of 7 fs. The pump beam was attenuated at 5 μJ per pulse with a spot size 2 mm in diameter at the sample cell where it was merged with the white probe pulse in a close angle (< 10°). The probe beam, after passing through the 2 mm sample cell, was focused on a 200 μm fiber optic cable that was connected to a CCD spectrograph (Ocean Optics, S2000-UV/Vis for the visible region and Horiba, CP-140 for the NIR region) for recording the time-resolved spectra ($\lambda = 420$–800 and 800–1200 nm). Typically, 5000 excitation pulses were averaged to obtain the transient spectrum at a set delay time. The kinetic traces at appropriate wavelengths were assembled from the time-resolved spectral data.

Measurements of nanosecond transient absorption spectra were performed according to the following procedure: A deaerated solution that contained the dyad was excited by a Panther OPO pumped by an Nd:YAG laser (Continuum, SLII-10, 4–6 ns fwhm) at $\lambda = 430$ nm. The photodynamics were monitored by continuous exposure to a xenon lamp (150 W) as a probe light and a photomultiplier tube (Hamamatsu 2949) as a detector. Transient spectra were recorded by using fresh solutions in each laser excitation. The solution was deoxygenated by purging with argon for 15 min prior to measurements being recorded.

Acknowledgements

This work is supported by the National Science Foundation (Grant 0453464 to F.D.), the donors of the Petroleum Research Fund administered by the American Chemical Society, a Grant-in-Aid (nos. 19205019 and 19750034 to K.O. and S.F.) from the Ministry of Education, Culture, Sports, Science, and Technology, Japan and CNRS (France).

---

[1] *The Photosynthetic Reaction Center*; (Eds.: J. Deisenhofer, J. R. Norris), Academic Press, San Diego, **1993**.

[2] a) M. R. Wasielewski, *Chem. Rev.* **1992**, *92*, 435; b) K. D. Jordan, M. N. Paddon-Row, *Chem. Rev.* **1992**, *92*, 395.

[3] a) D. Gust, T. A. Moore, *The Porphyrin Handbook, Vol. 8* (Eds.: K. M. Kadish, K. M. Smith, R. Guilard), Academic Press, San Diego, CA, **2000**, pp. 153–190; b) D. Gust, T. A. Moore, A. L. Moore, *Acc. Chem. Res.* **2001**, *34*, 40.

[4] a) S. Fukuzumi, D. M. Guldi, *Electron Transfer in Chemistry, Vol. 2* (Ed.: V. Balzani), Wiley-VCH, Weinheim, **2001**, pp. 270–337; b) H. Imahori, S. Fukuzumi, *Adv. Funct. Mater.* **2004**, *14*, 525; c) P. V. Kamat, *J. Phys. Chem. C* **2007**, *111*, 2834.

[5] F. D'Souza, O. Ito, *Coord. Chem. Rev.* **2005**, *249*, 1410.

[6] a) S. Fukuzumi, *Org. Biomol. Chem.* **2003**, *1*, 609; b) S. Fukuzumi, *Bull. Chem. Soc. Jpn.* **2006**, *79*, 177.

[7] T. Hasobe, H. Imahori, P. V. Kamat, T. K. Ahn, D. Kim, T. Hanada, T. Hirakawa, S. Fukuzumi, *J. Am. Chem. Soc.* **2005**, *127*, 1216.

[8] a) F. D'Souza, R. Chitta, S. Gadde, L. M. Rogers, P. A. Karr, M. E. Zandler, A. S. D. Sandanayaka, Y. Araki, O. Ito, *Chem. Eur. J.* **2007**, *13*, 916; b) F. D'Souza, S. Gadde, D.-M. I. Shafiqul, S.-C. Pang, A. L. Schumacher, M. E. Zandler, R. Horie, Y. Araki, O. Ito, *Chem. Commun.* **2007**, 480; c) F. D'Souza, R. Chitta, S. Gadde, D.-M. S. Islam, A. L. Schumacher, M. E. Zandler, Y. Araki, O. Ito, *J. Phys. Chem. B* **2006**, *110*, 25240.

[9] a) H. Imahori, D. M. Guldi, K. Tamaki, Y. Yoshida, C. Luo, Y. Sakata, S. Fukuzumi, *J. Am. Chem. Soc.* **2001**, *123*, 6617; b) H. Imahori, K. Tamaki, Y. Araki, Y. Sekiguchi, O. Ito, Y. Sakata, S. Fukuzumi, *J. Am. Chem. Soc.* **2002**, *124*, 5165; c) H. Imahori, Y. Sekiguchi, Y. Kashiwagi, T. Sato, Y. Araki, O. Ito, H. Yamada, S. Fukuzumi, *Chem. Eur. J.* **2004**, *10*, 3184.

[10] S. Fukuzumi, K. Ohkubo, H. Imahori, J. Shao, Z. Ou, G. Zheng, Y. Chen, R. K. Pandey, M. Fujitsuka, O. Ito, K. M. Kadish, *J. Am. Chem. Soc.* **2001**, *123*, 10676.

[11] H. Imahori, K. Tamaki, D. M. Guldi, C. Luo, M. Fujitsuka, O. Ito, Y. Sakata, S. Fukuzumi, *J. Am. Chem. Soc.* **2001**, *123*, 2607.

[12] K. Ohkubo, H. Kotani, J. Shao, Z. Ou, K. M. Kadish, Y. Chen, G. Zheng, R. K. Pandey, M. Fujitsuka, O. Ito, H. Imahori, S. Fukuzumi, *Angew. Chem.* **2004**, *116*, 871; *Angew. Chem. Int. Ed.* **2004**, *43*, 853.

[13] a) J. P. Bourgeois, F. Diederich, L. Echegoyen, J.-F. Nierengarten, *Helv. Chim. Acta*, **1998**, *81*, 1835; b) E. Dietel, A. Hirsch, E. Eichhorn, A. Rieker, S. Hachbarth, B. Roder, *Chem. Commun.* **1998**, *81*, 1835; c) N. Armaroli, G. Marconi, L. Echegoyen, J.-P. Bourgeois, F. Diederich, *Chem. Eur. J.* **2000**, *6*, 1629; d) D. M. Guldi, A. Hirsch, M. Scheloske, E. Dietel, A. Troisi, F. Zerbetto, M. Prato, *Chem. Eur. J.* **2003**, *9*, 4968.

[14] a) D. I. Schuster, P. Cheng, P. D. Jarowski, D. M. Guldi, C. Luo, L. Echegoyen, S. Pyo, A. R. Holzwarth, S. E. Braslavsky, R. M. Williams, G. Klihm, *J. Am. Chem. Soc.* **2004**, *126*, 7257; b) T. Galili, A. Regev, H. Levanon, D. I. Schuster, D. M. Guldi, *J. Phys. Chem. A* **2004**, *108*, 10632.

[15] a) P. A. Liddell, J. P. Sumida, A. N. Macpherson, L. Noss, G. R. Seely, K. N. Clark, A. L. Moore, T. A. Moore, D. Gust, *Photochem. Photobiol.* **1994**, *60*, 537; b) F. D'Souza, S. Gadde, M. E. Zandler, K. Arkady, M. E. El-Khouly, M. Fujitsuka, O. Ito, *J. Phys. Chem. A* **2002**, *106*, 12393; c) S. Fukuzumi, K. Okamoto, C. P. Gros, R. Guilard, *J. Am. Chem. Soc.* **2004**, *126*, 10441; d) S. Fukuzumi, K. Okamoto, Y. Tokuda, C. P. Gros, R. Guilard, *J. Am. Chem. Soc.* **2004**, *126*, 17059.

[16] a) Y. Deng, C. J. Chang, D. G. Nocera, *J. Am. Chem. Soc.* **2000**, *122*, 410; b) C. J. Chang, Y. Deng, C. Shi, C. K. Chang, F. C. Anson, D. G. Nocera, *Chem. Commun.* **2000**, 1355.

[17] J. T. Fletcher, M. J. Therien, *J. Am. Chem. Soc.* **2002**, *124*, 4298.

[18] K. M. Kadish, J. Shao, Z. Ou, L. Fremond, R. Zhan, F. Burdet, J.-M. Barbe, C. P. Gros, R. Guilard, *Inorg. Chem.* **2005**, *44*, 6744.

[19] a) M. Tanaka, K. Ohkubo, C. P. Gros, R. Guilard, S. Fukuzumi, *J. Am. Chem. Soc.* **2006**, *128*, 14625; b) C. P. Gros, F. Brisach, A. Theristoudi, E. Espinosa, R. Guilard, P. D. Harvey, *Inorg. Chem.* **2007**, *46*, 125; c) P. D. Harvey, C. Stern, C. P. Gros, R. Guilard, *Coord. Chem. Rev.* **2007**, *251*, 481.

[20] M. Maggini, G. Scorrono, M. Prato, *J. Am. Chem. Soc.* **1993**, *115*, 9798.

[21] a) H. Imahori, N. V. Tkachenko, V. Vehmanen, K. Tamaki, H. Lemmetyinen, Y. Sakata, S. Fukuzumi, *J. Phys. Chem. A* **2001**, *105*, 1750; b) N. V. Tkachenko, H. Lemmetyinen, J. Sonoda, K. Ohkubo, T. Sato, H. Imahori, S. S. Fukuzumi, *J. Phys. Chem. A* **2003**, *107*, 8834.

[22] a) P. D. W. Boyd, C. A. Reed, *Acc. Chem. Res.* **2005**, *38*, 235; b) A. L. Balch, M. M. Olmstead, M. M. *Coord. Chem. Rev.* **1999**, *185–186*, 601.

[23] a) For a review on applications of B3LYP/3-21G(*) method, see: M. E. Zandler, F. D'Souza, *C. R. Chim.* **2006**, *9*, 960, b) F. D'Souza, M. E. Zandler, P. M. Smith, G. R. Deviprasad, K. Arkady, M. Fujitsuka, O. Ito, *J. Phys. Chem. A* **2002**, *106*, 649; c) M. E. Zandler, P. M. Smith, M. Fujitsuka, O. Ito, F. D'Souza, *J. Org. Chem.* **2002**, *67*, 9122; d) M. E. El-Khouly, Y. Araki, O. Ito, S. Gadde, A. L. McCarty, P. A. Karr, M. E. Zandler, F. D'Souza, *Phys. Chem. Chem. Phys.* **2005**, *7*, 3163.

[24] D. Rehm, A. Weller, *Isr. J. Chem.* **1970**, *8*, 259.

[25] a) R. A. Marcus, N. Sutin, *Biochim. Biophys. Acta* **1985**, *811*, 265; b) R. A. Marcus, *Angew. Chem.* **1993**, *105*, 1161; *Angew. Chem. Int. Ed. Engl.* **1993**, *32*, 1111.

[26] K. Ohkubo, H. Imahori, J. Shao, Z. Ou, K. M. Kadish, Y. Chen, G. Zheng, R. K. Pandey, M. Fujitsuka, O. Ito, *J. Phys. Chem. A* **2002**, *106*, 10911.

[27] At 1000 ps, the singlet absorption at 1200 nm mostly disappears (Figure 8), whereas the absorption at 1000 nm due to the C_{60} radical anion still remains. This indicates that the C_{60} radical anion is formed via the porphyrin singlet excited state.

[28] For the Pacman effect on the excited-state dynamics of pillard cofacial bisporphyrins, see: C. J. Chang, Z.-H. Loh, Y. Deng, D. G. Nocera, *Inorg. Chem.* **2003**, *42*, 8262.

[29] H. Imahori, M. E. El-Khouly, M. Fujitsuka, O. Ito, Y. Sakata, S. Fukuzumi, *J. Phys. Chem. A* **2001**, *105*, 325.

[30] Gaussian 03, Revision B.04, M. J. Frisch, G. W. Trucks, H. B. Schlegel, G. E. Scuseria, M. A. Robb, J. R. Cheeseman, J. A. Montgomery Jr., T. Vreven, K. N. Kudin, J. C. Burant, J. M. Millam, S. S. Iyengar, J. Tomasi, V. Barone, B. Mennucci, M. Cossi, G. Scalmani, N. Rega, G. A. Petersson, H. Nakatsuji, M. Hada, M. Ehara, K. Toyota, R. Fukuda, J. Hasegawa, M. Ishida, T. Nakajima, Y. Honda, O. Kitao, H. Nakai, M. Klene, X. Li, J. E. Knox, H. P. Hratchian, J. B. Cross, V. Bakken, C. Adamo, J. Jaramillo, R. Gomperts, R. E. Stratmann, O. Yazyev, A. J. Austin, R. Cammi, C. Pomelli, J. W. Ochterski, P. Y. Ayala, K. Morokuma, G. A. Voth, P. Salvador, J. J. Dannenberg, V. G. Zakrzewski, S. Dapprich, A. D. Daniels, M. C. Strain, O. Farkas, D. K. Malick, A. D. Rabuck, K. Raghavachari, J. B. Foresman, J. V. Ortiz, Q. Cui, A. G. Baboul, S. Clifford, J. Cioslowski, B. B. Stefanov, G. Liu, A. Liashenko, P. Piskorz, I. Komaromi, R. L. Martin, D. J. Fox, T. Keith, M. A. Al-Laham, C. Y. Peng, A. Nanayakkara, M. Challacombe, P. M. W. Gill, B. Johnson, W. Chen, M. W. Wong, C. Gonzalez, J. A. Pople, Gaussian, Inc., Wallingford CT, **2004**.

Received: June 19, 2007